Journal of Chemical and Petroleum Engineering (JChPE)
Print ISSN: 2423-673X Online ISSN: 2423-6721

The Comprehensive Evaluation of the Coke Formation and Catalyst Deactivation in the Propane Dehydrogenation Reactor: Computational Fluid Dynamics Modelling

Soleiman Mosleh*, Parviz Darvishi

1. Department of Gas and Petroleum, Yasouj University, Gachsaran, Iran. E-mail: mosleh@yu.ac.ir
2. Department of Chemical Engineering, School of Engineering, Yasouj University, Yasouj, Iran. E-mail: pdarvishi@yu.ac.ir

ARTICLE INFO

Article History:
Received: 12 July 2022
Revised: 14 October 2022
Accepted: 18 October 2022

Article type: Research

Keywords:
CFD Modeling,
Coke Formation,
Deactivation,
Hot Spots,
Propane dehydrogenation

ABSTRACT

A numerical evaluation was performed to find out the impact of bed geometry on the catalyst deactivation and propane dehydrogenation efficiency by consideration of the coke formation in the reactor. Furthermore, the temperature distribution and propane conversion along the reactor were studied. The governing equations with appropriate initial and boundary conditions were solved numerically, while two different bed arrangements (i.e., rectangular and parallelogram) were evaluated to find the optimized geometry in order to avoid the creation of hot spots. Findings indicated that parallelogram arrangement causes more conversion percentage owing to more axial as well as the radial mixing of reactants compared to the rectangular arrangement. Moreover, the obtained numerical results revealed that the optimum operating temperature to achieve the maximum conversion is 550 °C. As the temperature rises from 450 ºC to 650 ºC, the conversion of propane increases from 68.15% to 99.51%, during the reactor length. When the temperature exceeds the optimum operating temperature, hot spots are created due to coke formation and also accumulation of coke on the catalyst bed surface that will lead to the deactivation of catalysts. The results of this work can be useful to examine the effects of operating conditions to understand better physical and chemical phenomena occurring in the propane dehydrogenation reactor.

Introduction

Propylene (C_3H_6) is well-known as an important petrochemical feedstock that is used for the fabrication of precious products such as polypropylene, acrylonitrile, cumene, propylene oxide, acrylic acid polypropylene, and acrylonitrile [1-3]. Over the past two decades, the increasing request for propylene derivatives caused increase in the propylene production demand. In this regard, different production techniques have been studied and developed [2,4]. Although the dehydrogenation of propane (C_3H_8) to propylene is a common and effective commercialized process, it suffers from some limitations, including thermodynamic restrictions on conversion, strong endothermicity, side reactions, and coke formation [5-8].

Owing to the thermodynamics restrictions, a high conversion percentage needs high temperatures which raises energy consumption. In this condition, the probability of coke formation increases owing to high temperature [9]. The coke formation leads to catalyst deactivation as well as creation of hot spots [10]; Hence, catalytic bed must be regenerated

* Corresponding Author: S. Mosleh (E-mail address: mosleh@yu.ac.ir)

Journal of Chemical and Petroleum Engineering, 2022, 56(2): 287- 301.
Publisher: University of Tehran, College of Engineering *DOI: 10.22059/JCHPE.2022.345525.1395*

periodically to remove the deposited carbon which imposes serious unit operating cost. It is worth noting that in the case of hot spots being closer to the reactor wall, serious damages will arise [11,12]. Accordingly, finding the optimized operating temperature is an essential step in the propane dehydrogenation process to overcome the mentioned limitations [13, 14].

The empirical studies for finding optimum conditions require high operating time and consume much reagents, which imposes a high cost on the process [15-17]. Hence, theoretical modeling based on the reaction kinetics, transport phenomena, operating conditions, and geometrical considerations could be a cost-effective approach for the prediction of reactor behavior [18]. Kamlesh Ghodasara et al. [19] developed mathematical model for catalytic propane dehydrogenation using a moving bed reactor while the reactor efficiency was assessed as a function of the operating parameter. In their research, different geometries were studied through the optimization of operating parameters, while propane conversion was examined as the response. Bijan Barghi et al. [20] proposed a mathematical model for propane dehydrogenation using an industrial catalyst to describe catalyst deactivation. Their findings showed that the addition of water and methanol as oxygenated additives could enhance the propane conversion while the coke formation is reduced. Seyed M. Miraboutalebi et al. [11] presented a numerical model for the kinetics of propane dehydrogenation using a radial-flow reactor. Pt-Sn/Al_2O_3 was applied as the catalyst, while the catalyst activity and propane conversion were evaluated as the responses. Their obtained numerical results revealed that the catalyst activity was highly time-dependent. Antonio Ricca et al. [2] used a mathematical approach for modeling a membrane-assisted propane dehydrogenation process, while catalyst activity and stability were considered as responses at two operating temperatures. Their Findings indicated a good agreement between experimental data and the results of the proposed kinetic model. Yun Jin et al. [5] developed a one-dimensional, steady-state model for propane dehydrogenation process. A hollow fiber membrane reactor was used, whereas the membrane area, fiber length, and flow rate was selected as the operational parameters. The obtained modeling results revealed that the optimum propylene selectivity was 91% at the operating temperature of 1000 °C when propane conversion reached 58%.

Although different modeling and correlations have been assessed for predicting propane conversion and temperature gradient during the propane dehydrogenation process, such correlations have disadvantages in terms of insufficient accuracy [20-25]. Therefore, this work focuses on the application of the computational fluid dynamics (CFD) technique for the examination of propane dehydrogenation reactors involving rector geometry, momentum, mass transfer, heat transfer, and reactions. Besides experimental studies, successful implementation of the CFD technique has been developed to evaluate overall reactor performance and coke deposition behaviors. Behnam and Dixon [26] examined the local carbon formation in the steam methane reforming process using a 3D-CFD model. Their proposed model showed a non-uniform descending carbon formation rate from the heated tube wall to the tube center. Xuesong Yang et al. [27] established a particle-resolved model for the investigation of coke formation. It was reported that the coke formation and catalyst deactivation are higher near the reactor wall. Claudio Antonio et al. [28] investigated the influence of hydrodynamics on activity and selectivity. Their findings showed that the optimum temperature was 453 °C, while the process efficiency increased from 6.0% to 6.7% for the 2D proposed model, and from 6.0% to 7% for the 3D proposed model. Furthermore, the selectivity increased from 20% to 26% and 21% for the 2D and 3D models, respectively. Gopal Manoharan and Buwa [29] developed a CFD model to understand the impact of various catalytic geometries on catalyst deactivation. Their research highlighted the quantitative relationship between the catalytic structure and the reactor performance.

The creation of changes in the bed structure leads to changes in transport rates and the catalyst loading in the reactor. The present work provides a developed model of transport in packed bed reactors and helps to a better understanding of the influence of reactor bed geometry on the reactor efficiency, and thereby aids in selecting the optimal configuration.

The present work provides a comprehensive evaluation to predict the product conversion, catalyst deactivation and creation of hot spots across the catalytic bed, with a reduction in the time and cost of the analysis. Different catalytic bed arrangements were modeled to the prediction of the product conversion, catalyst deactivation as well as temperature distribution across the bed. The finite element procedure was applied to solve all governing equations, including momentum, mass, and energy, with appropriate initial and boundary conditions along with the side reactions simultaneously. It is worth noting that few mathematical and CFD models have been presented in the recent literature on catalyst deactivation and the creation of hot spots. In contrast, in this work, an appropriate model has been proposed for the investigation of propane dehydrogenation system behavior. Generally, the current model covers many lacks of previously reported modeling.

Model Development

Geometrical Model

A two-dimensional CFD model was applied to evaluate the impact of temperature variations on the coke deposition and catalyst deactivation in the propane dehydrogenation reactor. An axial symmetry model was used for the simulation of a fixed bed reactor with a length of 0.15 m and a diameter of 0.02 m, while the bed was filled by spherical catalysts with a diameter of 0.001 m. The feed was entranced from the bottom of the reactor, passing through the catalytic bed and after conversion to the product, exited the reactor. The plug flow model was considered to describe the occurring chemical reactions. The geometry of the catalytic bed reactor for different bed geometries is illustrated in Fig. 1a.

Reaction kinetics

Since the propane dehydrogenation reaction is an endothermic equilibrium limited reaction, the high temperatures and low pressures are desirable in order to increase the yield reaction. However, it is essential to mention that high temperatures can cause undesirable side reactions which produce unwanted products. Hence, finding an optimized temperature is very necessary for such a process. The process reactions are mentioned as follows which Reaction. 1 is the main, while others are side reactions [30].

$$C_3H_8 \leftrightarrow C_3H_6 + H_2 \qquad \Delta H_1 = 124\ kJ/mol \tag{1}$$

Cracking reaction:

$$C_3H_8 \rightarrow CH_4 + C_2H_4 \qquad \Delta H_2 = 81\ kJ/mol \tag{2}$$

Ethylene hydrogenation:

$$C_2H_4 + H_2 \rightarrow C_2H_6 \qquad \Delta H_3 = -137\ kJ/mol \tag{3}$$

The proposed reaction rates for primary and side reactions were provided as follows [11]:

$$-r_1 = \frac{k_1\left(P_{C3H8} - \left(\frac{P_{C3H6}\,P_{H2}}{k_{eq}}\right)\right)}{1 + \left(\frac{P_{C3H6}}{k_{C3H6}}\right)} \tag{4}$$

$$-r_2 = k_2 P_{C3H8} \tag{5}$$

$$-r_3 = k_3 P_{C2H4}\,P_{H2} \tag{6}$$

where, r_i ($\frac{kmol}{m^3.s}$) is the reaction rate, k_i (s^{-1}) is the reaction rate constant, and P_i is the partial pressure of species. The reaction rate is given based on rector volume. The fixed bed volume fraction was considered 0.65.

Deactivation Model

The deactivation model was selected based on the rate of coke formation during the process (versus the time). The deactivation was estimated as follows [19, 20]:

$$\frac{dC_C}{dt} = \frac{dC_m}{dt} \tag{7}$$

where C_m is the coke concentration in monolayer described as follows [11]:

$$C_m = C_{max}^2\left(\frac{k_{1C}t}{1 + C_{max}k_{1C}t}\right) \tag{8}$$

The catalyst activity reduction due to monolayer–multilayer coke formation was estimated as follows [23]:

$$\alpha = (1 - \alpha_1 C_m)^2 \tag{9}$$

where α_1 indicates that the primary active surface, while C_m is the coke production rate due to reaction.

The reaction constants were calculated based on the Arrhenius equation chemical kinetics as follows [31]:

$$\mathrm{k_1} = \mathrm{k_{01}}\exp\left[\frac{-\mathrm{E_{a1}}}{\mathrm{R}\left(\left(\frac{1}{\mathrm{T}}\right) - \left(\frac{1}{\mathrm{T_0}}\right)\right)}\right] \tag{10}$$

$$\mathrm{k_2} = \mathrm{k_{02}}\exp\left[\frac{-\mathrm{E_{a2}}}{\mathrm{R}\left(\left(\frac{1}{\mathrm{T}}\right) - \left(\frac{1}{\mathrm{T_0}}\right)\right)}\right] \tag{11}$$

$$\mathrm{k_3} = \mathrm{k_{03}}\exp\left[\frac{-\mathrm{E_{a3}}}{\mathrm{R}\left(\left(\frac{1}{\mathrm{T}}\right) - \left(\frac{1}{\mathrm{T_0}}\right)\right)}\right] \tag{12}$$

$$k_{C3H6} = k_0\exp\left[\frac{-\Delta H}{R\left(\left(\frac{1}{T}\right) - \left(\frac{1}{T_0}\right)\right)}\right] \tag{13}$$

$$k_{eq} = k_{0e}\exp\left[\frac{-E_{eq}}{R\left(\left(\frac{1}{T}\right) - \left(\frac{1}{T_0}\right)\right)}\right] \tag{14}$$

$$k_{1c} = k_{01c}\exp\left[\frac{-E_{a1c}}{RT}\right] \tag{15}$$

$$k_{2c} = k_{02c}\exp\left[\frac{-E_{a2c}}{RT}\right] \tag{16}$$

The reaction kinetic parameters and their values are presented in Table 1.

Table 1. The values of kinetic parameters [11,23].

Parameter	Value	Unit
k_{01}	0.5242	(mmol/gr. min. bar)
k_{02}	0.00465	(mmol/gr. min. bar)
k_{03}	0.000236	(mmol/gr. min. bar)
k_{0}	3.46	(mmol/gr. min. bar)
k_{0e}	35.50	(mmol/gr. min. bar)
E_{a1}	34.57	(kJ/mol)
E_{a2}	137.31	(kJ/mol)
E_{a3}	154.54	(kJ/mol)
E_{eq}	35.50	(kJ/mole)
ΔH	-85.817	(kJ/mol)
α_1	813	g catalyst/g coke
C_{max}	0.000682	mg coke/mg catalyst
k_{01c}	234	mg coke/mg catalyst
E_{a1c}	38.43	kJ/mole
k_{02c}	0.00000145	mg coke/mg catalyst
E_{a2c}	125.51	kJ/mol

A "sequential steady-state solutions" technique has been used to compute the time-dependent manner of deactivating catalyst particles. Nevertheless, this simplified approach was very costly due to computation time. It should be noticed that more accurate modeling would be even more expensive, as the system of equations is very stiff, owing to the slow diffusion inside the catalysts particles. For assessment of the coke formation inside the catalyst particles, the time evolution of the carbon deposits was tracked by running a steady-state simulation. In this procedure, computation is performed at base case (un-deactivated) conditions to gain the initial local carbon deposition rates (r_{i0}). After that, over a time interval, the accumulating local carbon is calculated. Generally, the deactivation rate is estimated as follows [29]:

$$r_i = r_{i0}\exp\left(-\alpha C_c\right) \tag{17}$$

The Eq. 17 is applied to modify the reaction rates with fresh catalyst r_{i0} to give the reaction rates after 1 min. C_C (kmol/m^3) denotes the accumulated coke concentration on the catalyst. The CFD simulation was done at the steady-sated condition for a further 1-min period with the new reaction rates to gain the increased values of $C_{C,}$ and the process was then repeated.

Governing Equations

The kinetic equations of the main and side reactions along with the governing transport phenomena equations, including momentum, mass, and energy with appropriate initial and boundary conditions, were solved numerically.

Momentum transfer

The continuity and Navier-Stokes equations were applied throughout the reactor domain to the description of the flow of fluids as follows [27]:

$$\frac{\partial \rho}{\partial t} + \nabla \cdot (\rho \mathbf{u}) = 0 \tag{18}$$

$$\rho \frac{\partial \mathbf{u}}{\partial t} + \rho(\mathbf{u} \cdot \nabla)\mathbf{u} = -\nabla \cdot [-p\mathbf{I} + \mathbf{K}] + \mathbf{F} \tag{19}$$

where, ρ ($\frac{kg}{m^3}$) is density, u (m/s) is the velocity vector, P (Pa) is the total pressure, I denotes the identity matrix, and F ($\frac{N}{m^3}$) is the volumetric force vector.

Mass transfer

The mass transfer for each species throughout the reactor domain was given as follows [27]:

$$\rho\frac{\partial\omega_i}{\partial t}-\nabla\left(\rho D_{i.j}\nabla\omega_i+\rho D_{i.j}\frac{\nabla M_n}{M_n}-\rho\omega_i\sum_k\frac{M_i}{M_n}D_{i.j}\nabla x_k\right)+\rho(\mathbf{u}\cdot\nabla)\omega_i=0 \quad (20)$$

where, $D_{i.j}$ ($\frac{m^2}{s}$) is the diffusion coefficient of species.

Heat transfer

Energy balance equation throughout the reactor domain can be considered as follows [27]:

$$\rho C_P\frac{\partial T}{\partial t}+\rho C_P\mathbf{u}\cdot\nabla T+\nabla\cdot(-k\nabla T)=0 \quad (21)$$

where, C_P (*kJ/kg. K*) refers to the specific heat and *k* (*W/m. k*) denotes the thermal conductivity. The rate of production/consumption for all chemical components was obtained using the stoichiometry of the reactions, while the heat production term was calculated by multiplying the reaction rate by the heat generated by each reaction.

Solution technique

The proposed CFD model was solved using the finite element procedure. All partial differential equations, including mass transfer, momentum, and energy equations, were solved simultaneously with appropriate initial and boundary conditions. The numerical simulation was made with unstructured grids composed of approximately 163,000 nodes (including 1,156,000 tetrahedral cells by consideration the independency of their solution). Additionally, a higher density of elements was created in the regions close to the particles and the reactor wall. The convergence was certified by checking the scaled residuals to a criterion of 10^{-4} for the continuity and momentum, and 10^{-5} for the concentration factors. Fig. 2a shows the diagram of the sequence of steps that is used in this study. As can be seen, a comprehensive evaluation has been performed, including the pre-processing, simulations, post-processing results, and visualization. The boundary conditions were provided as follows:

At the reactor inlet: $C_i = C_{i0}, T = T_0, u = u_0$
At the reactor outlet: *Convective flux*, $p = p_0$
Axial symmetry: $\frac{\partial C_i}{\partial r} = 0$, $\frac{\partial T}{\partial r} = 0$
At the wall: $\frac{\partial C_i}{\partial r} = 0$, $-K\frac{\partial T}{\partial r} = U\,(T - T_c)$, $u=0$

The negligible internal mass- and energy-transport limitations were considered inside the catalyst particles. Furthermore, negligible external mass and heat transfer resistances were assumed at the surface of the catalyst particles. Moreover, the ideal gas law was supposed to describe the behavior of the gas phase inside the reactor.

Results and discussion

The evaluation of the temperature effect on the propane conversion revealed that higher operating temperatures lead to increasing propane conversion owing to the endothermic reaction (Fig. 1a).

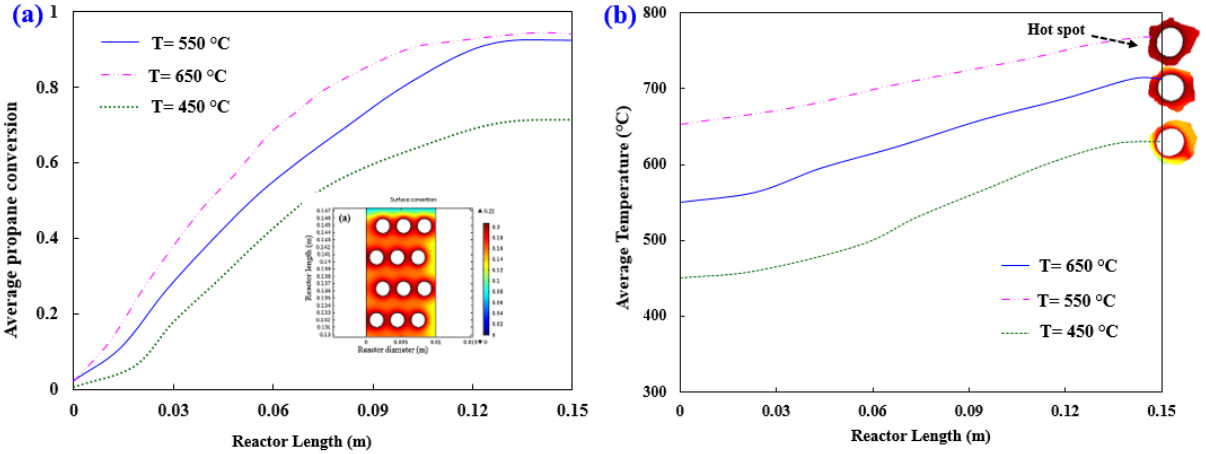

Fig. 1. The average propane conversion (a) and the average temperature (b) along the reactor obtained from the proposed CFD model

In fact, both reaction rates and species diffusivities are depending on temperature, hence increasing the temperature affects the propane conversion significantly. However, it should be noted that excessive temperature in the reactor has some disadvantages such as creating hot spots in the catalyst bed, which leads to the deactivation and ultimately destruction of the catalysts. In this condition, the system requires a catalyst revive cycle, which imposes serious unit operating costs, and in the case of that hot spots being closer to the reactor wall, serious damages will arise. Moreover, high temperature means a magnification of side reactions that causes a reduction of product purity. In this regard, finding the optimized temperature is an essential step in the propane dehydrogenation process. Typically, the impact of the operating temperature on the average temperature across the catalyst bed (Fig. 1b) indicated that the higher operating temperature causes high-temperature variation in the reactor length. Findings indicated that the maximum operating temperature to achieve the highest conversion without the formation of hot spots is 550 °C. The temperature gradually increases from the reactor entrance, and heat accumulation causes temperature rise especially in the final catalyst rows. When the operating temperature exceeds the optimum value, the temperature rises on the catalyst surface, which creates hot spots, especially in the final part of the reactor that will cause catalyst destruction as well as damage to the reactor structure.

A comparison of the average temperature for both bed geometries is shown in Fig. 2a.

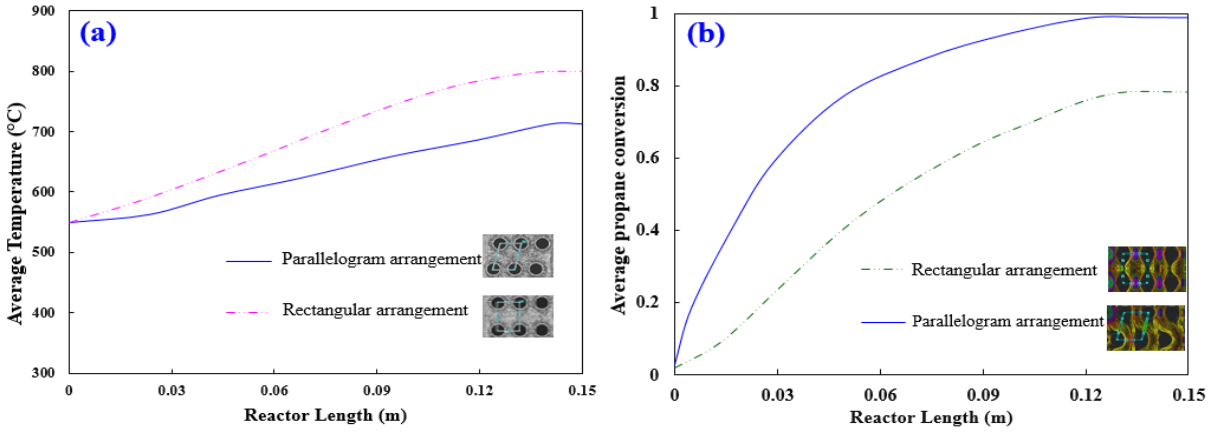

Fig. 2. Average temperature (a) and the average propane conversion (b) across the reactor at optimum condition (T=550 °C), obtained from the proposed CFD model

The different temperature gradient observed during the reactor length for rectangular and parallelogram arrangements shows an increase in the accumulated coke due to the continuous creation of coke for both bed geometries. As can be seen, the rate of increased temperature is considerably higher for the rectangular arrangement, which can be related to the accumulated coke. The accumulated coke decreases on the end part of the reactor length for both geometries. This is owing to decreasing in the reaction rates caused by less desirable. Findings can be analyzed as follows: rectangular arrangement contains higher accumulated coke compared to the parallelogram arrangement, which is owing to the higher reaction rates as a result of better flow distribution. In other words, the parallelogram arrangement creates better mixing which improves the conversion rate. The investigations to find the optimum catalyst bed arrangement revealed that the parallelogram arrangement significantly increases propane conversion in comparison to the rectangular arrangement (Fig. 2b), which would be related to the flow pattern through the bed.

In the case of the rectangular arrangement, reactants flow axially among the catalysts particle, while in the parallelogram arrangement, the reactants flow both axially and radially due to obstacles in their path. Under this condition, more mixing is occurred compared to the rectangular arrangement and consequently leads to more interactions between the reactants (Fig. 3). The obtained results for propane conversion at different parts of the reactor indicated that by crossing the catalytic bed conversion was increased gradually until reaches the maximum at reactor outlet owing to the consumption of raw materials. Temperature gradients in different parts of the reactor at optimal operating temperature revealed that the temperature increases throughout the reactor. At the entrance of the reactor, the heat is used to improve the reaction rate due to the endothermic reaction and by crossing the catalytic bed, the reaction rate gradually decreases owing to the consumption of raw materials. Therefore, the existing heat results in increasing the temperature at the end of the reactor.

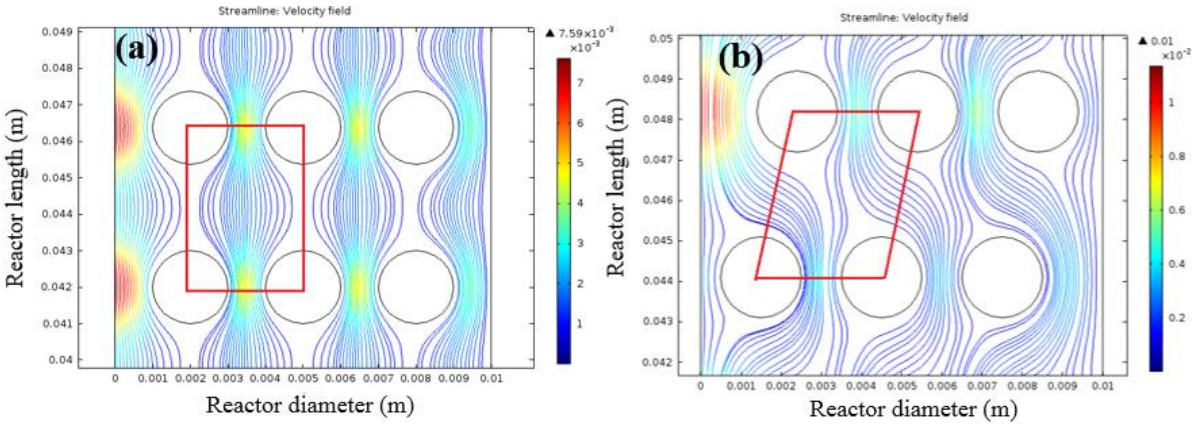

Fig. 3. Streamlines of the velocity field in the catalytic bed at optimum condition (T=550 °C). (a): rectangular arrangement, (b): parallelogram arrangement obtained from the proposed CFD model

The comparison of the propane conversion for both bed geometries under the same conditions shows that the parallelogram arrangement beings more efficiently (Fig. 4). As can be seen, in the parallelogram arrangement, the conversion is formed more uniformly, while the rectangular arrangement causes less product purity.

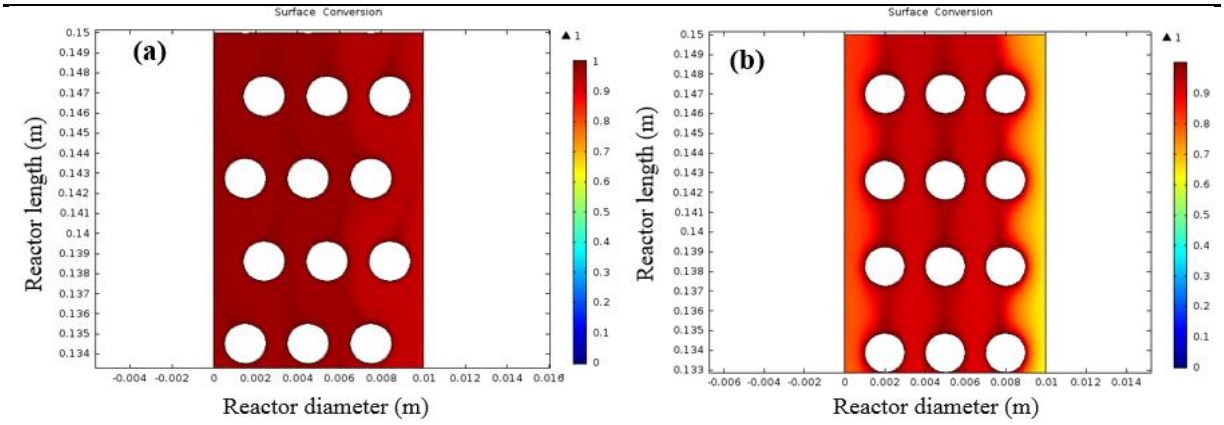

Fig. 4. The propane conversion at the reactor height of 0.15 m at optimum condition (T=550 °*C*). (a): parallelogram arrangement, (b): rectangular arrangement

In the rectangular arrangement, the conversion rate is very slow at the entrance of the reactor, while using the parallelogram arrangement, the conversion rate was improved because of better mixing as well as good distribution of the reactants in the reactor (Fig. 5).

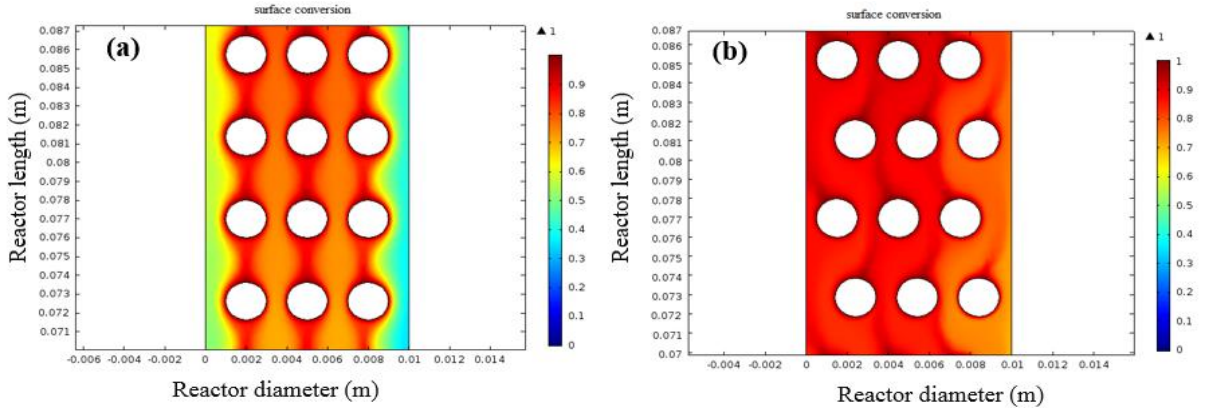

Fig. 5. The propane conversion at the reactor height of 0.087 m at optimum condition (T=550 °*C*). (a): rectangular arrangement, (b): parallelogram arrangement

The deactivation model results demonstrated that due to the coke formation on the catalytic bed and, consequently, deactivation of the catalysts active surfaces, the propane conversion falls by half the usual amount (Fig. 6). Moreover, the propane concentration gradient across the reactor length at different times indicated that the conversion rate is more uniform using the parallelogram arrangement (Fig. 7). The reaction rate was higher near the catalyst surfaces. As time increases, owing to more carbon deposition and consequently higher deactivation rates, the reaction rate is reduced. In fact, the coke deposition directly affects the catalytic bed activity.

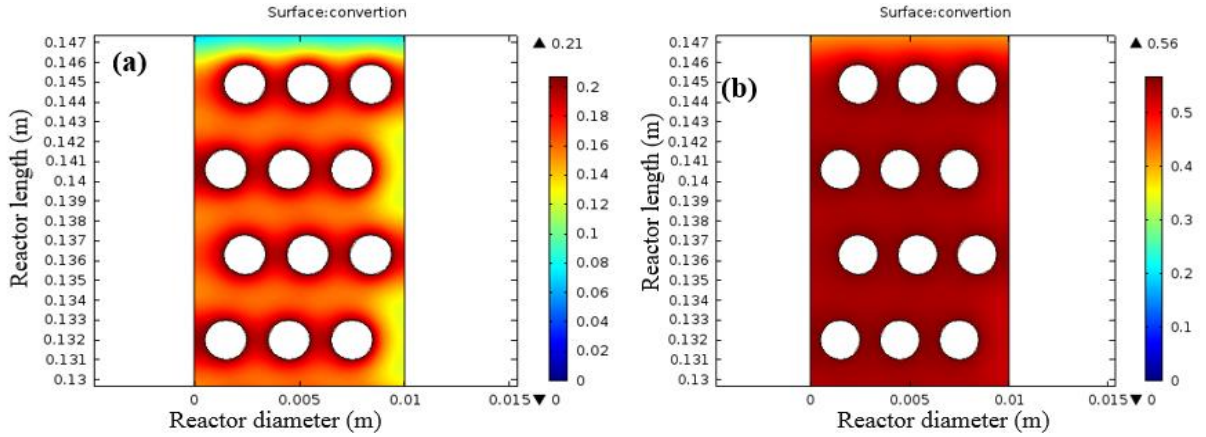

Fig. 6. The propane conversion at the reactor height of 0.147 m for parallelogram arrangement at optimum condition (T=550 °*C*), (a): at the time of 1600 s, (b): at the time of 400 s

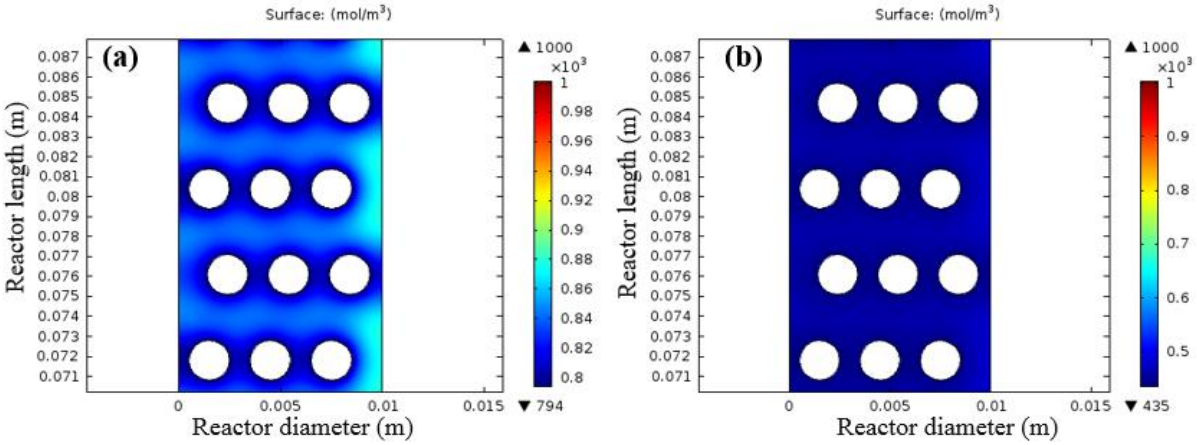

Fig. 7. The propane concentration at the reactor height of 0.087 m for parallelogram arrangement at optimum condition (T=550 °*C*), (a): at the time of 1600 s (b): at the time of 400 s

The carbon concentration gradient across the reactor length at different times (Fig. 8) revealed that at first, high propane concentration causes more coke formation, while by reduction in the propane concentration during the process, the coke formation rate decreases.

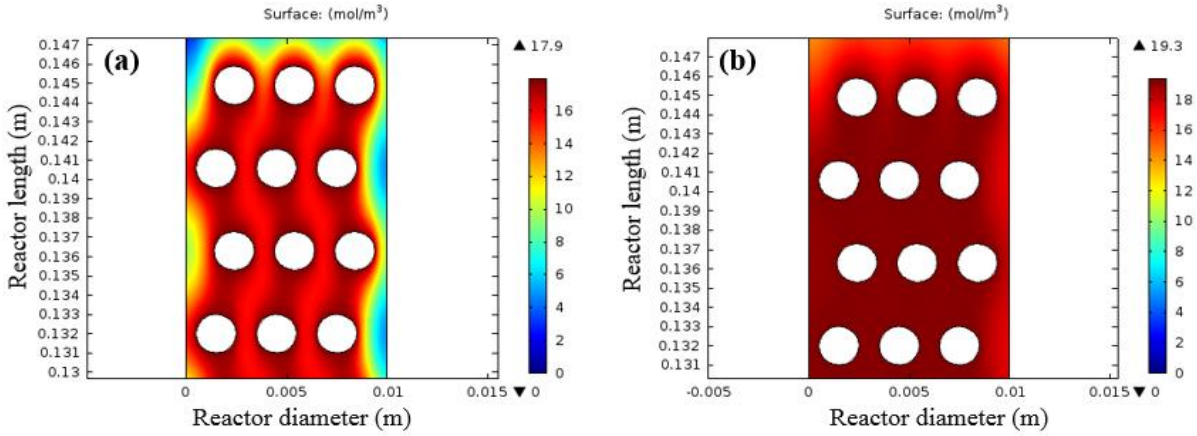

Fig. 8. The carbon concentration at the reactor height of 0.15 m at optimum condition (T=550 °*C*). (a): parallelogram arrangement and the time of 400 s, (b): parallelogram arrangement and the time of 1600s

The variation of the coke formation rates versus the time at different reactor temperatures is represented in Fig. 9. An extreme impact of the reaction temperature is seen. At 550℃, after longer times on stream, the coke formation rate maintains at a constant value. Hence this temperature is an optimum condition.

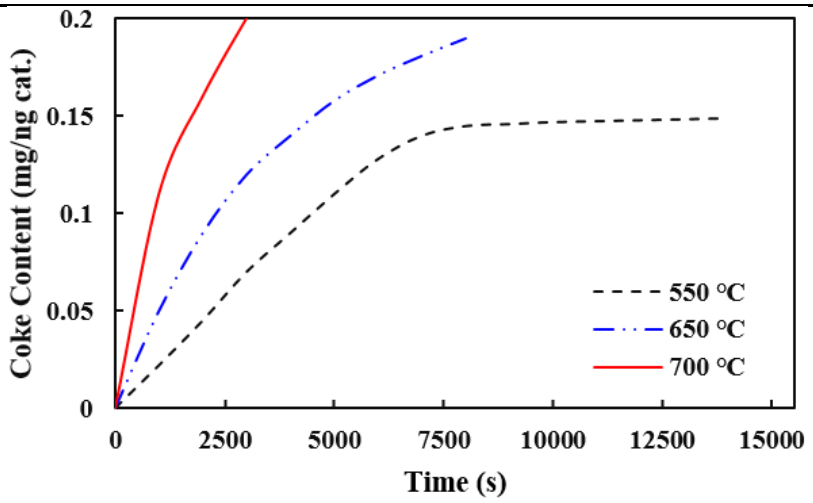

Fig. 9. Coke content versus time at different reactor temperatures

The propane conversion percentage across the reactor length for parallelogram arrangement with and without deactivation model was studied (Fig. 10), and the obtained results showed that propane dehydrogenation process modeling is very unreasonable regardless of the coke production reaction, so it is very necessary to consider the deactivation equation in the process modeling.

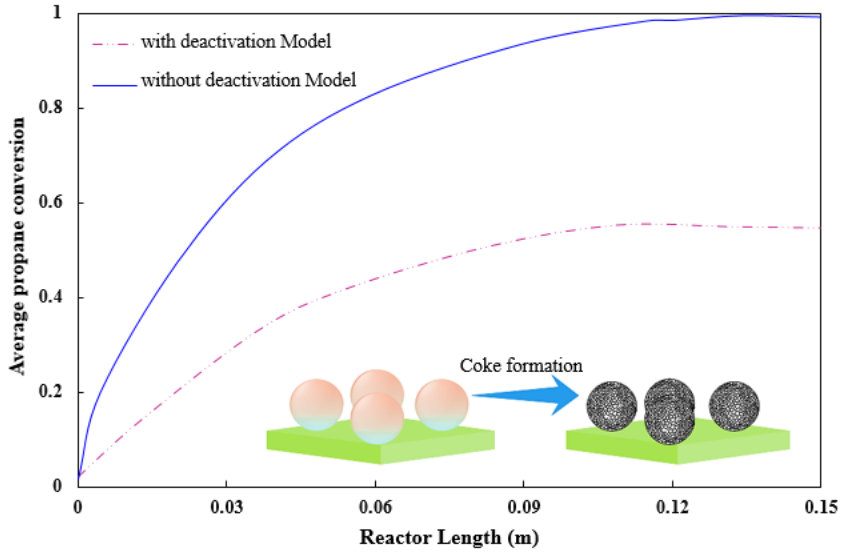

Fig. 10. The comparison of the propane conversion percentage along the reactor at optimum condition (T=550 *°C*), with and without deactivation model

The tracer test was carried out to investigate the mixing performance of both bed configurations. The tracer with a specified mass fraction was initially patched at the reactor inlet, while a transient CFD simulation was used to analysis of the improvement of mixing performance. The simulation results for both bed arrangements were depicted using Fig. 11. It can be concluded that the parallelogram arrangement causes more mixing inside the reactor.

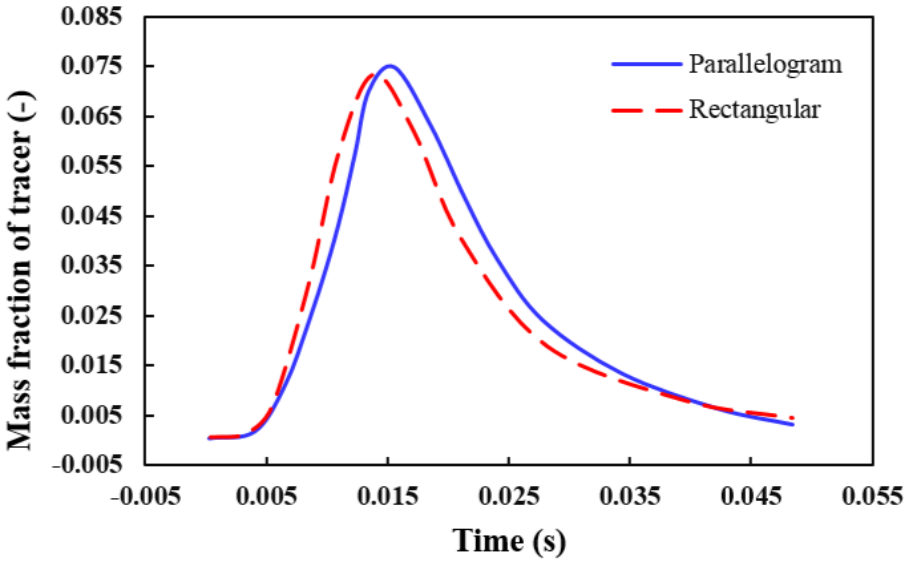

Fig. 11. The tracer test for both bed configurations

Validation of the model was evaluated using experimental data from Hamel et al. [32]. Fig. 12 shows the propylene selectivity (%) versus propane conversion (%) for both proposed model results and empirical data. The propane conversion (X) and propylene selectivity (S) were obtained as follows [33]:

$$X\ (\%) = \frac{F_{propane}^{In} - F_{propane}^{Out}}{F_{propane}^{In}} \times 100 \quad (22)$$

$$S\ (\%) = \frac{F_{propylene}^{Out}}{F_{propane}^{In} - F_{propane}^{Out}} \times 100 \quad (23)$$

where F denoted the molar flow. As shown in Fig. 12, the difference between experimental data and proposed model results is within 10%, which confirms the validation of the proposed model.

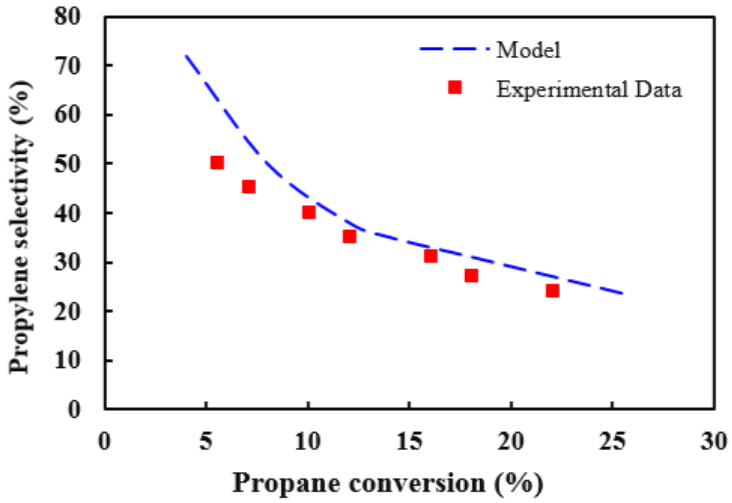

Fig. 12. The proposed model validation: comparison of the obtained models results vs. experimental data

Conclusion

A CFD model was applied to the analysis of the catalytic bed reactor for the propane dehydrogenation process. The effect of operating temperature on the propane conversion, creation of hot spots, and deactivation of the bed was evaluated. Findings revealed that higher operating temperatures lead to increasing propane conversion owing to the endothermic reaction. However, it should be noted that excessive temperature in the reactor has some disadvantages, such as creating hot spots in the catalyst bed, which leads to the deactivation and ultimately destruction of the catalysts. Accordingly, the optimal operating temperature to achieve the highest conversion without forming hot spots was found at 550 °C. To comprehend further the differences in temperature variation for different bed geometries, a comparison of the temperature distribution on the catalyst surfaces was performed. Findings indicated that the propane conversion decreases exponentially related to the increase in catalyst deactivation with the reactor length. The rectangular arrangement brings faster deactivation of the catalysts compared to the parallelogram arrangement. This phenomenon is more detrimental to the catalyst volume near the reactor wall as it may create local spots, which is a serious danger for wall failure

Acknowledgment

The authors are grateful for financial support from the Research Council of the University of Yasouj.

Nomenclature

C_i	The chemical concentration of species ($\frac{mol}{m^3}$)
C_m	The coke concentration in monolayer ($\frac{mol}{m^3}$)
C_P	The specific heat ($kJ/kg.\ K$)
D_i	The diffusion coefficient of species ($\frac{m^2}{s}$)
F	The volumetric force vector ($\frac{N}{m^3}$)
I	The identity matrix
k	The thermal conductivity ($W/m.\ k$)
k_i	The reaction rate constant (s^{-1})
P	The total pressure (Pa)
P_i	The partial pressure of species (Pa)
R_i	The reaction rate ($\frac{kmol}{m^3.s}$)
T	The absolute temperature (K)
u	The velocity vector (m/s)
X_{C3H8}	Propane conversion
α	Catalyst activity
ρ	Density ($\frac{kg}{m^3}$)
μ	The dynamic viscosity $\left(\frac{Ns}{m^2}\right)$

References

[1] Choi SW, Sholl DS, Nair S, Moore JS, Liu Y, Dixit RS, Pendergast JG. Modeling and process simulation of hollow fiber membrane reactor systems for propane dehydrogenation. AIChE Journal. 20; 63:4519-4531.

[2] Ricca A, Montella F, Iaquaniello G, Palo E, Salladini A, Palma V. Membrane assisted propane dehydrogenation: Experimental investigation and mathematical modelling of catalytic reactions. Catalysis Today. 2019; 331:43-52.
[3] Lian Z, Ali S, Liu T, Si C, Li B, Su DS. Revealing the Janus character of the coke precursor in the propane direct dehydrogenation on Pt catalysts from a kMC simulation. ACS Catalysis. 2018; 8:4694-4704.
[4] Du Y, Zhang L, Berrouk AS. Exergy analysis of propane dehydrogenation in a fluidized bed reactor: Experiment and MP-PIC simulation. Energy Conversion and Management. 2019; 202:112213.
[5] Jin Y, Meng X, Bo M, Yang N, Sunarso J, Liu S. Parametric modeling study of oxidative dehydrogenation of propane in La0. 6Sr0. 4Co0. 2Fe0. 8O3-δ hollow fiber membrane reactor. Catalysis Today. 2019; 330:135-141.
[6] Zhu Y, An Z, Song H, Xiang X, Yan W, He J. Lattice-confined Sn (IV/II) stabilizing raft-like Pt clusters: high selectivity and durability in propane dehydrogenation. ACS catalysis. 2017; 710:6973-6978.
[7] Sheintuch M, Nekhamkina O. Architecture alternatives for propane dehydrogenation in a membrane reactor. Chemical Engineering Journal. 2018; 347:900-12.
[8] Saerens S, Sabbe MK, Galvita VV, Redekop EA, Reyniers MF, Marin GB. The positive role of hydrogen on the dehydrogenation of propane on Pt (111). ACS catalysis. 2017; 7:7495-508.
[9] Jiang F, Zeng L, Li S, Liu G, Wang S, Gong J. Propane dehydrogenation over Pt/TiO2–Al2O3 catalysts. ACS catalysis. 2015; 5:438-447.
[10] Tian J, Lin J, Xu M, Wan S, Lin J, Wang Y. Hexagonal boron nitride catalyst in a fixed-bed reactor for exothermic propane oxidation dehydrogenation. Chemical Engineering Science. 2018; 186:142-151.
[11] Miraboutalebi SM, Vafajoo L, Kazemeini M, Fattahi M. Simulation of Propane Dehydrogenation to Propylene in a Radial-Flow Reactor over Pt-Sn/Al2O3 as the Catalyst. Chemical Engineering & Technology. 2015; 38:2198-2206.
[12] Han Z, Li S, Jiang F, Wang T, Ma X, Gong J. Propane dehydrogenation over Pt–Cu bimetallic catalysts: the nature of coke deposition and the role of copper. Nanoscale. 2014; 6:10000-10008.
[13] Ricca A, Palma V, Iaquaniello G, Palo E, Salladini A. Highly selective propylene production in a membrane assisted catalytic propane dehydrogenation. Chemical Engineering Journal. 2017; 330:1119-1127.
[14] Shen LL, Xia K, Lang WZ, Chu LF, Yan X, Guo YJ. The effects of calcination temperature of support on PtIn/Mg (Al) O catalysts for propane dehydrogenation reaction. Chemical Engineering Journal. 2017; 324:336-346.
[15] Chen C, Zhang J, Zhang B, Yu C, Peng F, Su D. Revealing the enhanced catalytic activity of nitrogen-doped carbon nanotubes for oxidative dehydrogenation of propane. Chemical Communications journal. 2013; 49:8151-8153.
[16] Yang ML, Zhu J, Zhu YA, Sui ZJ, Yu YD, Zhou XG, Chen D. Tuning selectivity and stability in propane dehydrogenation by shaping Pt particles: A combined experimental and DFT study. Journal of Molecular Catalysis. 2014; 395:329-236.
[17] Fattahi M, Kazemeini M, Khorasheh F, Rashidi A. Kinetic modeling of oxidative dehydrogenation of propane (ODHP) over a vanadium–graphene catalyst: Application of the DOE and ANN methodologies. Journal of Industrial and Engineering Chemistry. 2014; 20:2236-2247.
[18] Karthik GM, Buwa VV. Effect of particle shape on catalyst deactivation using particle-resolved CFD simulations. Chemical Engineering Journal. 2019; 377:120164.
[19] Ghodasara K, Hwang S, Smith R. Catalytic propane dehydrogenation: Advanced strategies for the analysis and design of moving bed reactors. Korean Journal of Chemical Engineering. 2015; 32(11):2169-2180.

[20] Barghi B, Fattahi M, Khorasheh F. Kinetic modeling of propane dehydrogenation over an industrial catalyst in the presence of oxygenated compounds. Reaction Kinetics, Mechanisms and Catalysis. 2012; 107:141-155.
[21] Gascón J, Téllez C, Herguido J, Menéndez M. Propane dehydrogenation over a Cr2O3/Al2O3 catalyst: transient kinetic modeling of propene and coke formation. Applied Catalysis. 2003; 248:105-116.
[22] Li Q, Sui Z, Zhou X, Chen D. Kinetics of propane dehydrogenation over Pt–Sn/Al2O3 catalyst. Applied Catalysis. 2011; 398:18-26.
[23] Lobera MP, Tellez C, Herguido J, Menéndez M. Transient kinetic modelling of propane dehydrogenation over a Pt–Sn–K/Al2O3 catalyst. Applied Catalysis. 2008; 349:156-164.
[24] Zhang Y, Zhou Y, Qiu A, Wang Y, Xu Y, Wu P. Effect of alumina binder on catalytic performance of PtSnNa/ZSM-5 catalyst for propane dehydrogenation. Industrial & Engineering Chemistry Research. 2006; 45:2213-2219.
[25] Rozanska X, Fortrie R, Sauer J. Oxidative dehydrogenation of propane by monomeric vanadium oxide sites on silica support. The Journal of Physical Chemistry. 2007; 111:6041-6050.
[26] Behnam M, Dixon A. 3D CFD simulations of local carbon formation in steam methane reforming catalyst particles. International Journal of Chemical Reactor Engineering. 2017; 15 :6.
[27] Yang X, Wang S, Zhang K, He Y. Evaluation of coke deposition in catalyst particles using particle-resolved CFD model. Chemical Engineering Science. 2021; 229:116122.
[28] Reyes-Antonio C.A, Cordero M.E, Pérez-Pastenes H, Uribe S, Al-Dahhan M. Analysis of the effect of hydrodynamics over the activity and selectivity of the oxidative dehydrogenation of propane process in a packed bed reactor through CFD techniques. Fuel. 2020; 280:118510.
[29] Gopal Manoharan K, Buwa V.V. Structure-resolved CFD simulations of different catalytic structures in a packed bed. Industrial & Engineering Chemistry Research. 2019; 58:22363-22375.
[30] Shelepova EV, Vedyagin AA, Mishakov IV, Noskov AS. Mathematical modeling of the propane dehydrogenation process in the catalytic membrane reactor. Chemical Engineering Journal. 2001; 176:151-157.
[31] Chin SY, Hisyam A, Prasetiawan H. Modeling and simulation study of an industrial radial moving bed reactor for propane dehydrogenation process. International Journal of Chemical Reactor Engineering. 2016; 14:33-44.
[32] Hamel C, Tóta Á, Klose F, Tsotsas E, Seidel-Morgenstern A. Analysis of single and multi-stage membrane reactors for the oxidation of short-chain alkanes—Simulation study and pilot scale experiments. Chemical Engineering Research and Design. 2008; 86: 753-764.
[33] Sheintuch M, Liron O, Ricca A, Palma V. Propane dehydrogenation kinetics on supported Pt catalyst. Applied Catalysis A: General. 2016; 516: 17-29.Steefel CI. CrunchFlow. Softw. Model. Multicomponent React. Flow Transp. User's Man. . Lawrence Berkeley Natl Lab, Berkeley USA. 2009.

How to cite: Mosleh S, Darvishi P. The Comprehensive Evaluation of the Coke Formation and Catalyst Deactivation in the Propane Dehydrogenation Reactor: Computational Fluid Dynamics Modelling. Journal of Chemical and Petroleum Engineering. 2022; 56(2): 287-301.